IJAMS Peer reviewed journal
International Journal of Applied Mathematics and Simulation

PV-Battery hybrid system power management based on backstepping control.

[1]Aimen Acil MAANANI, [2]Yacine MAANANI, 3rd Achour Betka [3], 4th AymenBenguessoum[4]

https://doi.org/10.69717/ijams.v1.i2.102

Abstract-With the increasing global energy consumption and the need for sustainable solutions, this article focuses on the energy management of a hybrid photovoltaic (PV)-battery system using the backstepping method. The research addresses the challenges of intermittent solar irradiation by implementing an incremental conductance maximum power point tracking (MPPT) algorithm for the PV panel and backstepping control for battery charging and discharging. The system's performance and control effectiveness were validated throughlaboratory experiments. The results demonstrate the system's robustness, stability, and ability to respond to fast changes, making it a promising solution for efficient energy management in hybrid PV-battery systems. The findings provide valuable insights for future research and advancements in this field.

Keywords: Energy management, Hybrid PV/battery system, Backstepping method, PV panels-Batteries-DC/DC boost converter, DC/DC bidirectional converter, Incremental conductance MPPT, Renewable energies, Energy storage-nonlinear control, experimental validation.

I. INTRODUCTION

Renewable energies are an alternative way to conventional fossil fuels, and they originate from natural phenomena caused by the sun and the earth. The six primary sources of renewable energy are solar, wind, hydro, geothermal, marine, and biomass. The potential of these sources depends on various factors like sunshine, wind exposure, topology, and land geometry [1]. To cover the load demand in arid zones, solar based devices are generally combined with storage elements to get Hybrid systems. The PV-battery hybrid system combines a photovoltaic (PV) panel with a battery storage element to increase the autonomy of the system,

In the literature, there are different types of energy systems (isolated energy systems, connected energy systems, single-source energy systems, and multi-source energy systems). In general, the term Hybrid Energy System (HES) refers to electric power generation systems that use multiple types ofsources in order to combine the advantages of each while taking into account their respective specifications. These hybrid sources combine very high specific energy and maximum power available for considerable durations. Today, the use of hybrid energy systems (HES) has advanced in several industrial sectors such as embedded systems (automobiles, airplanes, boats, etc.) as well as for powering isolated communities or even those connected to grids[11].

[1]LGEB Laboratory of Electrical Engineering of Biskra, Mohamed Khider University, Biskra, Algeria
Maanani.aimenacil@gmail.com
[2]LGEB Laboratory of Electrical Engineering of Biskra, Mohamed Khider University, Biskra, Algeria
yacine.maanani@gmail.com
[3]LGEB Laboratory of Electrical Engineering of Biskra, Mohamed Khider University, Biskra, Algeria
betkaachour@gmail.com
[4]LGEB Laboratory of Electrical Engineering of Biskra, Mohamed Khider University, Biskra, Algeria
aymenbeng2000@gmail.com

Communicated Editor: Nabil khelfallah

***Manuscript received** Dec 06,2023; **revised** May 19, 2024; **accepted** Nov 27, 2024; **published** Dec 28, 2024.*

II. PV-BATTERY HYBRID SYSTEM

Effective management strategies require an understanding of the behavior of a system in response to input data, and this understanding is achieved through a prior numerical simulation, based on an explicit modeling of the process, the first step is modeling the involved sources, which are the PV panel and the lead-acid battery, and then going in an analog way to a mathematical representation of the static converters, of the types of DC-DC boost and DC-DC buck-boost converters. The acquired models are essential for comprehending and enhancing the system's overall performance to harness its full potential and ensure stability in real-world scenarios.

In the framework of this study, a PV-battery hybrid system, which supplies a stationary load is presented in ’Fig .1" To permit an effective control and power management of the system, each source is equipped with a side DC-DC converter. An optimal operation of the PV panel is guaranteed via a quite adjusting of the related duty cycle. In the same point of view, the battery side converter is a Bidirectional DC-DC converter, which permits charging and discharging current of the battery.

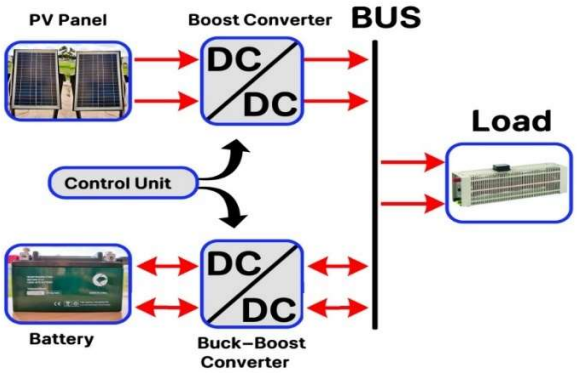

Figure 1.Synoptic scheme of the hybrid system

III. MODELINGOF SOURCES

A.PV Panel Model

Photovoltaic (PV) panels convert sunlight directly into electricity through the photovoltaic effect.
PV models range varies from simple single-diode models to complex multi-diode models. The selection of an appropriate model depends on the required accuracy and computational effort. The single-diode model, due to its balance between complexity and accuracy, is widely used in PV system design and simulation [2].
Photovoltaic panels are considered neither voltage nor current sources, but they can be estimated as voltage-controlled current generators, where the implicit four-parameter model (I_{pv}, R_s, V_{th}, and I_o) reflects the current-voltage characteristic with notable accuracy:

$$I_{pv} = I_{cc} - I_o \left[exp\left(\frac{V_{pv}+R_s.I_{pv}}{V_{th}}\right) - 1 \right] \quad (1)$$

This characteristic can be illustrated by the equivalent diagram (Fig.2) [14-15]; consisting of a variable current generator, mounted in parallel with a diode D characterizing the junction and a resistance Rs (series resistance) representing the losses by Joule effects.
The thermal voltage V_{th} and the diode saturation current Io are identified by:

$$I_o = (I_{cc} - I_{op}).exp[-\frac{V_{op}-R_s.I_{op}}{V_{th}}] \quad (2)$$

$$V_{th} = \frac{V_{op}+R_s.I_{op}-V_{oc}}{\log\left(1-\frac{I_{op}}{I_{cc}}\right)} \quad (3)$$

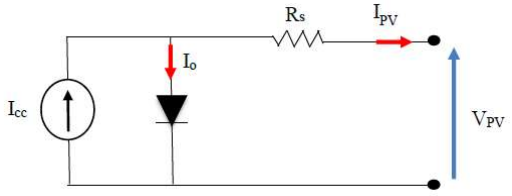

Figure 2. Equivalent diagram of the photovoltaic panel

IV. MODELING OF STATIC CONVERTERS

In the context of our study on 'Modelingof Static Converters,' we employ DC-DC boost converters and buck-boost converters in hybrid PV-battery systems. The average model simplifies analysis and facilitates control design, stability assessment, and energy management. The boost converter comprises a controlled switch, a flyback diode, and storage components (L, C), while Kirchhoff's laws aid in deriving average model equations for the buck-boost converter, enabling comprehensive system testing [13].

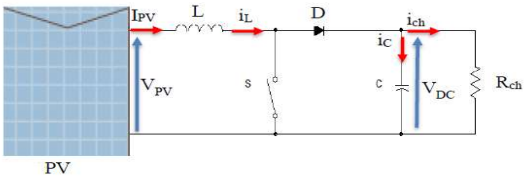

Figure 3. Descriptive diagram of the boost converter

A. Modeling of PV Panel Boost Converter

The average model for the PV panel boost converter is derived from the application of Kirchhoff's voltage and current laws (KVL and KCL) during the closed and open phases of the transistors [13]. This yields the following average model weighted bythe duty cycle α:

$$\begin{cases} \dot{x} = (A_1.x + B_1.Vpv).\alpha + (A_2.x + B_2.Vpv)(1-\alpha) \\ V_{dc} = [D_1.\alpha + D_2.(1-\alpha)].x \end{cases} \quad (4)$$

For this converter, the parameters are:

- Capacitance (C) = 2200 µF
- Inductance (L) = 15 mH
- Resistance (r) = 2.8 Ω

B. Modeling of Battery Buck-Boost Converter (Bidirectional Converter)

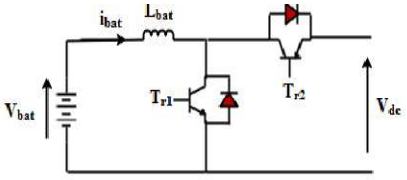

Figure 4. Converter associated with batteries.

Similarly, the average model for the battery buck-boost converter is obtained by applying Kirchhoff's voltage and current laws during the closed and open phases of the transistors, resulting in the following average model:

$$L_{bat}\frac{di_{bat}}{dt} = V_{bat} - (1-\alpha_{bat})V_{dc} \quad (5)$$

For this converter, the parameters are:

- Capacitance (C) = 2200 µF
- Inductance (L) = 12.21 mH
- Resistance (r) = 2.6 Ω

The model expressed in Equation (5) defines the battery's behavior during charging ($i_{bat} < 0$) and discharging ($i_{bat} > 0$), with switches Tr1 and Tr2 being complementary tuned, as presented in Equation (6):

$$\alpha_{Tr1} + \alpha_{Tr2} = 1 \quad (6)$$

V. CONTROL STRATEGIES FOR THE PV-BATTERY HYBRID SYSTEM

A. MPPT (Maximum Power Point Tracking) Algorithm

Maximum Power Point Tracking (MPPT) is a critical technology in photovoltaic (PV) systems. Its main purpose is to optimize power output by continuously tracking the Maximum Power Point (MPP), which varies with external factors like temperature and solar irradiation intensity. MPPT adjusts to these changing conditions, ensuring PV cells operate as close as possible to their MPP. This dynamic regulation maximizes power extraction, enhancing overall PV system efficiency. One widely used MPPT method is Incremental Conductance (IncCond)

B. The Incremental Conductance Method

The IncCond method, an advanced MPPT technique, computes the derivative of power with respect to voltage to pinpoint the MPP. By iteratively modifying the converter's duty cycle and adjusting the voltage, this method seeks the point where the derivative of power over voltage approaches zero, indicating the MPP. In "Fig 5", the flowchart of this technique is presented.

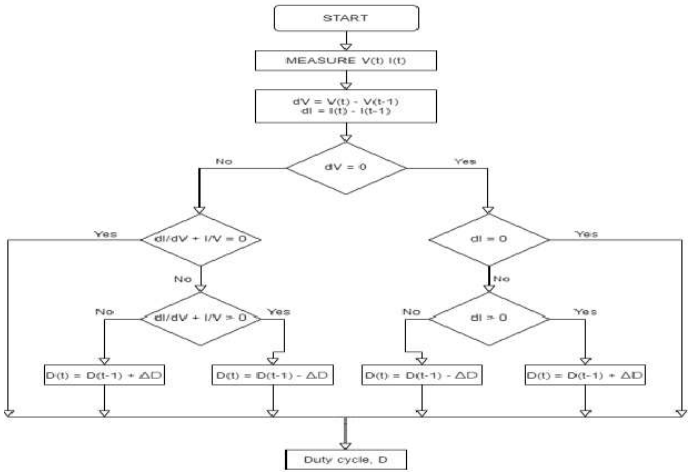

Figure 5. Flowchart of the IncCond MPPT Algorithm [12]

The algorithm hinges on the condition that the derivative of power (Ppv) with respect to voltage (Vpv) is zero at the maximum power point (MPP) and changes sign on either side of the MPP, represented by Equation (7).

$$\frac{dP_{pv}}{dV_{pv}} = 0 \qquad (7)$$

At the MPP, this equation can be explicitly expressed as a function of both PV voltage and current, as given by Equation (8).

$$V_{pv}\frac{dI_{pv}}{dV_{pv}} + I_{pv} = 0 (8)$$

The algorithm iteratively adjusts the converter's duty cycle, ensuring that dIpv/dVpv matches the absolute value of the instantaneous conductance Ipv/Vpv. This Incremental Conductance (IncCond) method excels in accuracy, rapid MPP detection, and steady-state oscillation elimination, enhancing energy efficiency.

IncCond is a practical choice for energy management in hybrid PV-Battery systems, selected based on specific system requirements and constraints. In this work, IncCond is utilized for PV side boost converter control, as depicted in the accompanying figure.

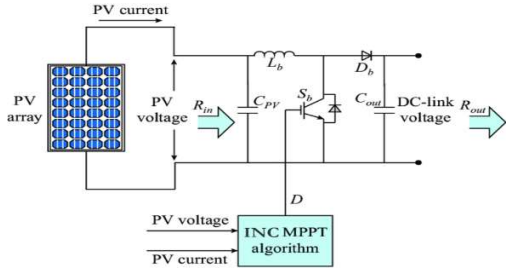

Figure 6. Synoptic Scheme of the Control of the PV Boost Converter [5]

VI. The Application of The Backstepping Method

A. In case of battery discharging:

The average model of the boost DC-DC converter is given as follows:

$$\begin{cases}\dot{x_1} = \frac{r}{L}x_1 - (1-u)\frac{x_2}{L} + \frac{E}{L} \\ \dot{x_2} = (1-u)\frac{x_1}{C} + \frac{I_{pvs}}{C} - \frac{x_2}{RC}\end{cases}(9)$$

Where the state vector is:$x = \begin{bmatrix} i_b \\ V_{dc} \end{bmatrix}$, and u is the converter duty cycle. In this model, I_{pvs} expresses the PV current on the DC bus side and is considered as a disturbance input. E denotes the battery voltage V_B.

1) Step One:

We first calculate the inductor current tracking error Z_1, given in (10). It is worth noting here that this choice is justified by the fact that the boost converter is an unstable non minimum phase system, and the deduction of the control law via the choice of the DC bus voltage tracking error as Z_1 fails. To overcome this situation, by choosing Z1 as (10), the dc bus voltage can be indirectly controlled[6].

$$Z_1 = x_1 - I_d(10)$$

Where the reference battery current I_d,is deduced through the power flow in steady state, as follows:

$$I_d = \frac{(\frac{V_{dc}^2}{R} - V_{PV}.I_{PV})}{E}(11)$$

And its derivative is:

$$\dot{Z_1} = \dot{x_1} - \dot{I_d} \ (12)$$

A first positive definite Lyapunov function is chosen as

$$V_1 = \frac{1}{2}Z_1^2(13)$$

By choosing the gradient of V_1 as semi-definite function, one gets:

$$\dot{Z_1} = -c_1Z_1(14)$$

Where c_1 is a manipulated positive constant.

Plugging $\dot{x_1}$ from equation (9) in equation (14):

$$\dot{Z_1} = -\frac{r}{L}x_1 - (1-u)\frac{x_2}{L} + \frac{E}{L} - \dot{I_d} = -c_1Z_1(15)$$

In this step, the stabilization part α_1 can be deduced as:

$$\alpha_1 = \frac{x_2}{L} = \frac{\left[c_1Z_1 - \frac{r}{L}x_1 + \frac{E}{L} - \dot{I_d}\right]}{(1-u)}(16)$$

2) Step Two:

In an analog way, the second error Z_2 is expressed as follows, which means that the DC bus voltage is regulated through the stabilization part α_1: [8]

$$Z_2 = \frac{x_2}{L} - \alpha_1 \quad => \frac{x_2}{L} = Z_2 + \alpha_1(17)$$

We replace $\frac{x_2}{L}$in equation (15) with equation (17), one gets:

$$\dot{Z_1} = -(1-u)[Z_2 + \alpha_1] - \frac{r}{L}x_1 + \frac{E}{L} - \dot{I_d}(18)$$

Plugging α_1 from equation (16) in equation (18) To finally get:

$$\dot{Z_1} = -c_1Z_1 - (1-u)Z_2(19)$$

The derivative α_1 can be explicitly given by:

$$\dot{\alpha_1} = \frac{\left[c_1\dot{Z_1} - \frac{r}{L}\dot{x_1} + \frac{\dot{E}}{L} - \ddot{I_d}\right](1-u)}{(1-u)^2} + \frac{\dot{u}\left[c_1Z_1 - \frac{r}{L}x_1 + \frac{E}{L} - \dot{I_d}\right]}{(1-u)^2}$$

(20)

$$\dot{\alpha_1} = \frac{-c_1^2Z_1 - c_1(1-u)Z_2 + \frac{r^2}{L^2}x_1 + (1-u)\frac{rx_2}{L^2} - \frac{rE}{L^2} + \frac{\dot{E}}{L} - \ddot{I_d} + \dot{u}\alpha_1}{(1-u)}(21)$$

We replace both $\dot{\alpha_1}$ and $\frac{\dot{x_2}}{L}$ in the derivative of Z_2 one obtains:

$$\dot{Z_2} = \frac{\dot{x_2}}{L} - \dot{\alpha_1} \quad (22)$$

$$\dot{Z_2} = (1-u)\frac{x_1}{LC} - \frac{x_2}{LRC} + \frac{\dot{i_{pvs}}}{LC} - \left[\frac{-c_1^2 Z_1 - c_1(1-u)Z_2 + \frac{r^2}{L^2}x_1 + (1-u)\frac{rx_2}{L^2} - \frac{rE}{L^2} + \frac{\dot{E}}{L} - \ddot{I_d} + \dot{u}\alpha_1}{(1-u)}\right] \quad (23)$$

In this second step, a new positive definite Lyapunov function, extended to the second tracking error is proposed as:

$$V_2 = \frac{1}{2}Z_1^2 + \frac{1}{2}Z_2^2 \quad (24)$$

$$\Rightarrow \dot{V_2} = Z_1\dot{Z_1} + Z_2\dot{Z_2} = Z_1[-C_1 Z_1 - Z_2(1-u)] + Z_2\dot{Z_2} \quad (25)$$

The convergence of both Z_1, and Z_2 to zero, imposes that the gradient of V_2 takes the following form:

$$\dot{V_2} = -\dot{c}_1 Z_1^2 - c_2 Z_2^2 \quad (26)$$

According to this conclusion, the following equality is deduced:

$$\dot{Z_2} - Z_1(1-u) + C_2 Z_2 = 0 \quad (27)$$

Plugging $\dot{Z_2}$ from equation (23) into equation (27):

$$(1-u)\frac{x_1}{LC} - \frac{x_2}{LRC} + \frac{\dot{i_{pvs}}}{LC} + \left[\frac{c_1^2 Z_1 + c_1(1-u)Z_2 - \frac{r^2}{L^2}x_1 - (1-u)\frac{rx_2}{L^2} + \frac{rE}{L^2} - \frac{\dot{E}}{L} + \ddot{I_d} - \dot{u}\alpha_1}{(1-u)}\right] - Z_1(1-u) + C_2 Z_2 = 0 \quad (28)$$

We extract $\dot{u}$ from equation (28) to finally have the control law of our system:

$$\dot{u} = \frac{\left[\begin{array}{c}[c1^2 - (1-u)^2]Z_1 + (c_1+c_2)(1-u)Z_2 + \ddot{I_d} + \left[\frac{(1-u)^2}{LC} - \frac{r^2}{L^2}\right]x_1 - (1-u)x_2\left[\frac{1}{RLC} + \frac{r}{L^2}\right] \\ + \frac{\dot{i_{pvs}}(1-u)}{LC} + \frac{rE}{L^2} - \frac{\dot{E}}{L}\end{array}\right]}{\alpha_1} \quad (29)$$

3) Zero Dynamics Study

The zero dynamics study focuses on the deduction of the steady state duty cycle, when both the tracking errors Z_1 and Z_2, as well as the control input gradient $\dot{u}$ tend to zero. A second order equation of the control law is obtained, having two possible roots, and as remarked, since the tolerable range of the duty cycle is between 0 and 1, only the following root u 2 is suitable[9]:

$$u_2 = 1 - \frac{1}{2}\left(-\frac{i_{pvs}}{x_1} - \left(\frac{1}{R} + \frac{r.C}{L}\right)\frac{x_2}{x_1} - \sqrt{\left(\frac{i_{pvs}}{x_1} - \left(\frac{1}{R} + \frac{r.C}{L}\right)\frac{x_2}{x_1}\right)^2 - \frac{4.(r.E - r^2 x_1).C}{L.x_1}}\right) \quad (30)$$

B. In case of battery charging:

The average model of the boost DC-DC converter is given as follows:

$$\begin{cases} \dot{x_1} = \frac{-r}{L}x_1 - \frac{x_2}{L} + u\frac{E}{L} \\ \dot{x_2} = \frac{x_1}{C} + \frac{I_{pvs}}{C} - \frac{x_2}{RC} \end{cases} \quad (31)$$

Where the state vector is: $x = \begin{bmatrix} i_b \\ V_{dc} \end{bmatrix}$, and u is the converter duty cycle. In this model, I_{pvs} expresses the PV current on the DC bus side, and is considered as a disturbance input. E denotes the battery voltage V_B.

1) Step One:

Firstly, the inductor current tracking error Z_1 is calculated, given in (32). It is worth noting here that this choice isfor the sake of continuity, because in the first scenario, Z_1 was given as the equation (10), therefore, Z_1 in this case is also given as (32).

$$Z_1 = x_1 - I_d \quad (32)$$

And its derivative is presented in the following equation and is plugged by $\dot{x_1}$:

$$\dot{Z_1} = \dot{x_1} - \dot{I_d} = \frac{-r}{L}x_1 + \frac{u.E}{L} - \frac{x_2}{L} - \dot{I_d} \quad (33)$$

Where the reference battery current I_d, is deduced through the power flow in steady state, as follows[7]:

$$I_d = \frac{(\frac{V_{dc}^2}{R} - V_{PV}.I_{PV})}{E} (34)$$

A first positive definite Lyapunov function is chosen as follows:

$$V_1 = \frac{1}{2} Z_1^2 (35)$$

By choosing the gradient of V_1 as semi-definite function, one gets:

$$\dot{Z_1} = -c_1 Z_1 (36)$$

Where c_1 is a manipulated positive constant.

Plugging $\dot{Z_1}$ from equation (32) in equation (36):

$$\dot{Z_1} = -\frac{r}{L} x_1 - \frac{x_2}{L} + \frac{u.E}{L} - \dot{I_d} = -c_1 Z_1 \quad (37)$$

In this step, the stabilization part α_1 can be deduced as:

$$\alpha_1 = \frac{x_2}{L} = c_1 Z_1 - \frac{r}{L} x_1 + \frac{u.E}{L} - \dot{I_d} \quad (38)$$

2) Step Two:

In an analog way, the second error Z_2 is expressed as follows, which means that the DC bus voltage is regulated through the stabilization part α_1[10]:

$$Z_2 = \frac{x_2}{L} - \alpha_1 \Rightarrow \frac{x_2}{L} = Z_2 + \alpha_1 (39)$$

We replace $\frac{x_2}{L}$ in equation (37) with equation (39), one gets:

$$\dot{Z_1} = -\frac{r}{L} x_1 - Z_2 - \alpha_1 + \frac{u.E}{L} - \dot{I_d} (40)$$

Plugging α_1 from equation (38) in equation (40) to finally get:

$$\dot{Z_1} = -c_1 Z_1 - Z_2 (41)$$

The derivative α_1 can be explicitly given by:

$$\dot{\alpha_1} = c_1 \dot{Z_1} - \frac{r}{L} \dot{x_1} + \frac{\dot{u}.E}{L} - \ddot{I_d} (42)$$

$$\dot{\alpha_1} = \frac{r^2}{L^2} x_1 - \frac{u.r.E}{L^2} + \frac{r}{L^2} x_2 + \frac{\dot{u}.E}{L} - \ddot{I_d} - c_1^2 Z_1 (43)$$

We replace both $\dot{\alpha_1}$ and $\frac{\dot{x_2}}{L}$ in the derivative of Z_2, one obtains:

$$\dot{Z_2} = \frac{\dot{x_2}}{L} - \dot{\alpha_1} (44)$$

$$\dot{Z_2} = \left[\frac{1}{C} - \frac{r^2}{L^2}\right] x_1 - \left[\frac{1}{RC} + \frac{r}{L^2}\right] x_2 + c_1^2 Z_1 + c_1 Z_2 + \frac{i_{pvs}}{C} + \frac{u.r.E}{L^2} - \frac{\dot{u}.E}{L} + \ddot{I_d} (45)$$

In this second step, a new positive definite Lyapunov function, extended to the second tracking error is proposed as:

$$V_2 = \frac{1}{2} Z_1^2 + \frac{1}{2} Z_2^2 (46)$$

$$\Rightarrow$$

$$\dot{V_2} = Z_1 \dot{Z_1} + Z_2 \dot{Z_2} = Z_1[-C_1 Z_1 - Z_2(1-u)] + Z_2 \dot{Z_2} (47)$$

The convergence of both Z_1, and Z_2 to zero, imposes that the gradient of V_2 takes the following form:

$$\dot{V_2} = -\dot{c_1} Z_1^2 - c_2 Z_2^2 (48)$$

According to this conclusion, the following equality is deduced:

$$\Rightarrow \dot{Z_2} - Z_1 + C_2 Z_2 = 0 (49)$$

Plugging $\dot{Z_2}$ from equation (45) into equation (50):

$$\left[\frac{1}{C} - \frac{r^2}{L^2}\right] x_1 - \left[\frac{1}{RC} + \frac{r}{L^2}\right] x_2 + c_1^2 Z_1 + c_1 Z_2 + \frac{i_{pvs}}{C} + \frac{u.r.E}{L^2} - \frac{\dot{u}.E}{L} + \ddot{I_d} - Z_1 + C_2 Z_2 = 0 (50)$$

We extract $\dot{u}$ from equation (50) to finally have the control law of our system:

$$\dot{u} = \frac{\left[\left[\frac{1}{C} - \frac{r^2}{L^2}\right] x_1 - \left[\frac{1}{RC} + \frac{r}{L^2}\right] x_2 + \frac{u.r.E}{L^2} + \frac{i_{pvs}}{C} + \ddot{I_d} + (c_1^2 - 1) Z_1 + (c_2 + c_2) Z_2\right]}{\frac{L}{E}}$$

(51)

3) Zero Dynamics study

The zero dynamics study focuses on the deduction of the steady state duty cycle, when both the tracking errors Z_1 and Z_2, as well as the control input gradient $\dot{u}$ tend to zero. Since the tolerable range of the duty cycle is between 0 and 1, an equation of the control law u is obtained:

$$u = \frac{-\left[\frac{1}{C}-\frac{r^2}{L^2}\right]x_1+\left[\frac{1}{RC}+\frac{r}{L^2}\right]x_2-\frac{i_{pvs}}{C}-\ddot{i}_d}{\frac{L^2}{r.E}} \quad (52)$$

The idea behind the deduction of this control law, is to avoid the saturation of the control law while using (51), caused mainly by the accumulation of errors, due to the imprecision of both voltage and current sensors.

C. logic commutation criteria

The choice of the bidirectional converter operation, whether to be a boost converter and discharge the battery or a buck converter and charge the battery depends on the sign of the reference battery current ($_{bref}$), which can be calculated using the next equation:

$$i_{bref} = \frac{\left[\frac{V_{dc}^2}{R}-P_{pv}\right]}{V_b} \quad (53)$$

As for the choice criteria itself, it's presented as follows:

$$\begin{cases} \text{if } i_{bref} > 0 \Rightarrow p_{ch} > P_{pv} \Rightarrow \textit{operate as boost} \\ \text{if } i_{bref} < 0 \Rightarrow p_{ch} < P_{pv} \Rightarrow \textit{operate as buck} \end{cases} \quad (54)$$

VII. Experimental Validation

To experimentally validate the control approaches, a small-scale hybrid system is assembled in the Renewable Energy Laboratory, where the implementation is performed using an Arduino Mega 2560 board. The explicit electronic scheme and the test bench is presented in **figure (7)**

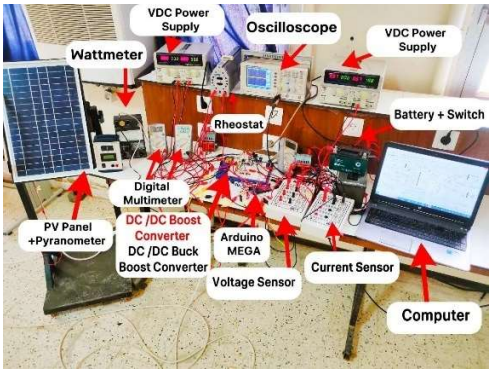

Figure 7: Picture of the Assembled Small-Scale Hybrid System in the RE Laboratory

The results of the backstepping-controlled boost converter are presented in this section, with a static load of R=20 Ω, and a reference voltage of V_{DCref}=25V

The obtained curves from testing the controller while discharging the battery are presented in the next figures.

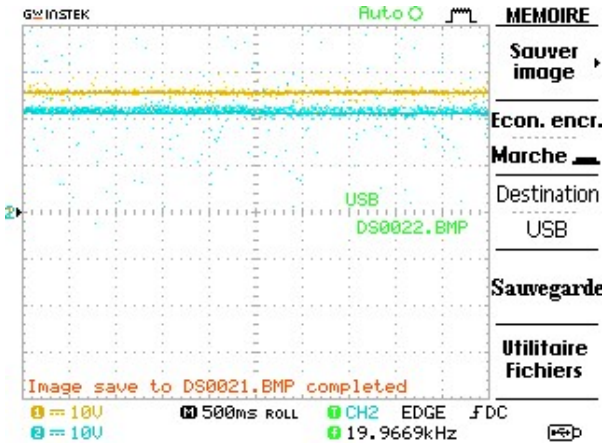

a) V_{DC} (blue) + V_{DCRef}(yellow)

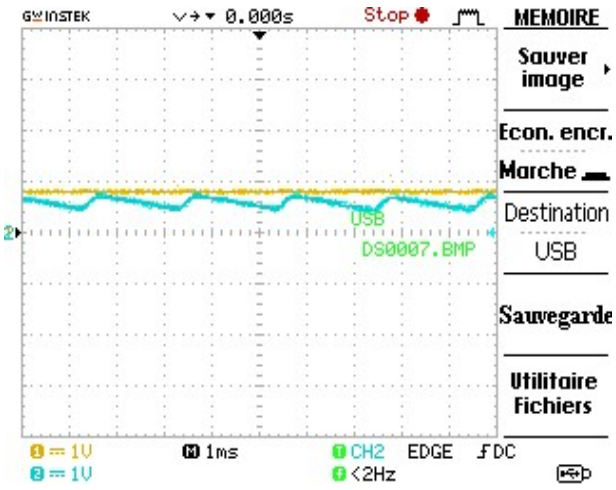

b) I_b(blue) + I_{bRef}(yellow)

Figure 8 : the obtained curves of the backstepping based controller :

V_{DC} ,V_{DCRef} , I_b, I_{bRef}.

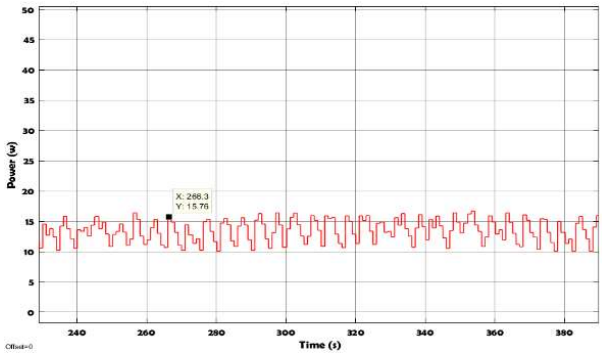

Figure 9 : the battery's power

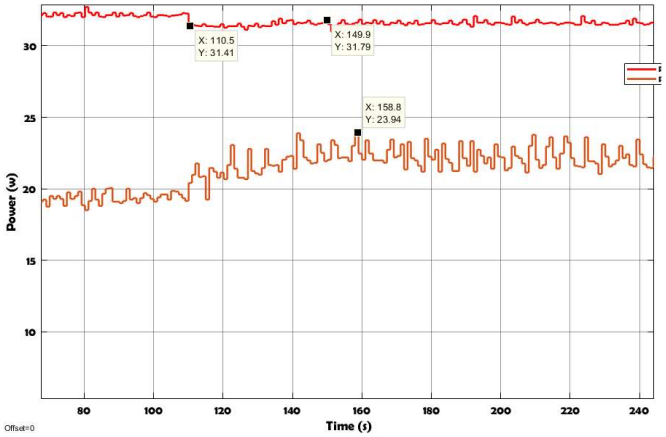

Figure 10: the load's power + the sum of the PV panel and the battery's power

The curves illustrate power management on the battery side using a backstepping-based controller via a boost DC-DC converter. The continuous bus voltage (VDC) stabilizes at VDC=21.5V, slightly below the reference value of 25V, showing a decrease of

approximately 3.5V. The battery current closely approaches the reference value (IbRef=0.64A), maintaining oscillations between Ibmax=0.64A and Ibmin=0.5A due to coil effects.

The combined power of the battery and PV panel fluctuates around Ptot=31W, matching the anticipated load power. However, the load's power hovers around Pch=23.5W, influenced by the reduced VDC. The PV panel's power oscillates around PPV=15W, while the battery's power compensates the load with a value around Pb=16W.

Overall, these curves demonstrate effective power management in the hybrid system by the controller

- Practical Obstacles

During the work on this article, several obstacles posed challenges and impeded the progress, resulting in limitations that affected the attainment of optimal outcomes. Some of these obstacles included:

-Faulty electrical and electronic components.

-Inadequate wiring leading to signal distortion and interference.

-The Arduino board's limited commutation frequency.

-The microcontroller's restricted processing capabilities.

To elaborate on the Arduino board's limitations, the PWM output frequency of the board is limited to f=490Hz, which is significantly lower than the required commutation frequency essential for achieving the desired system performance. This limited frequency range constrained our ability to accurately control and modulate the electrical signals, impacting the overall efficiency of the system.

VIII. CONCLUSON

Inthis research project, a PV-battery hybrid system was thoroughly investigated under the control of the nonlinear backstepping approach. Comprehensive insights into system components, models, and control laws were provided. Utilizing the Incremental Conductance MPPT algorithm with a DC-DC boost converter, power extraction from the solar panel was successfully optimized. Bus voltage regulation and battery control were effectively implemented using the backstepping method with a buck-boost converter, accommodating both discharging and charging modes. Simulations have demonstrated the effectiveness, responsiveness, robustness, and stability of the system and controls. It's acknowledged that experimental validation was limited to the discharging phase due to time constraints. Future work should encompass further experimental testing for a more comprehensive assessment.

REFERENCES

[1] MAAMIR, Madiha. *Techniques de supervision d'énergie d'un système d'entrainement Electrique hybride*. 2020. Thèse de doctorat. Université Mohamed Khider–Biskra. Search in Google Scholar, View

[2] DE SOTO, Widalys, KLEIN, Sanford A., et BECKMAN, William A. Improvement and validation of a model for photovoltaic array performance. *Solar energy*, 2006, vol. 80, no 1, p. 78-88. Search in Google Scholar, https://doi.org/10.1016/j.solener.2005.06.010

[3] ERICKSON, Robert W. et MAKSIMOVIC, Dragan. *Fundamentals of power electronics*. Springer Science & Business Media, 2007. Search in Google Scholar, View

[4] JYOTHI, Vellanki Mehar, MUNI, T. Vijay, *et al.* An optimal energy management system for pv/battery standalone system. *International Journal of Electrical and Computer Engineering*, 2016, vol. 6, no 6, p. 2538. Search in Google Scholar, View Article

[5] KUMAR, Vinit et SINGH, Mukesh. Derated mode of power generation in PV system using modified perturb and observe MPPT algorithm. *Journal of Modern Power Systems and Clean Energy*, 2020, vol. 9, no 5, p. 1183-1192. Search in Google Scholar, https://doi.org/10.35833/MPCE.2019.000258

[6] MOURAD, Loucif. *Synthèse de lois de commande non-linéaires pour le contrôle d'une machine asynchrone à double alimentation dédiée à un système aérogénérateur*. 2016. Thèse de doctorat. Ph. D. thesis, Université Aboubakr Belkaid–Tlemcen–Faculté de Technologie. Search in Google Scholar, View

[8] AMARA, Karima, MALEK, Ali, BAKIR, Toufik, *et al.* Adaptive neuro-fuzzy inference system based maximum power point tracking for stand-alone photovoltaic system. *International Journal of Modelling, Identification and Control*, 2019, vol. 33, no 4, p. 311-321. Search in Google Scholar, https://doi.org/10.1504/IJMIC.2019.107480

[9] RAHMAN, Sumaiya et RAHMAN, Hasimah Abdul. Use of photovoltaics in microgrid as energy source and control method using MATLAB/Simulink. *International Journal of Electrical and Computer Engineering*, 2016, vol. 6, no 2, p. 851. Search in Google Scholar, View Article

[10] ABD ALLAH, Boucetta et DJAMEL, Labed. Control of power and voltage of solar grid connected. *Bulletin of Electrical Engineering and Informatics*, 2016, vol. 5, no 1, p. 37-44. Search in Google Scholar, https://doi.org/10.11591/eei.v5i1.519